

Electronic Supplementary Material**A unique dual-shell encapsulated structure design achieves stable and high-rate lithium storage of Si@a-TiO₂@a-C anode**

Guang Ma*, Chong Xu (✉)*, Dongyuan Zhang, Sai Che, Yuxin Liu, Gong Cheng, Chenlin Wang, Kexin Wei, and Yongfeng Li (✉)

State Key Laboratory of Heavy Oil Processing, China University of Petroleum, Beijing 102249, China

E-mails: chongxu@cup.edu.cn (C.X.), yfli@cup.edu.cn (Y.L.)

* G.M. and C.X. contributed equally to this work and should be considered as co-first authors.

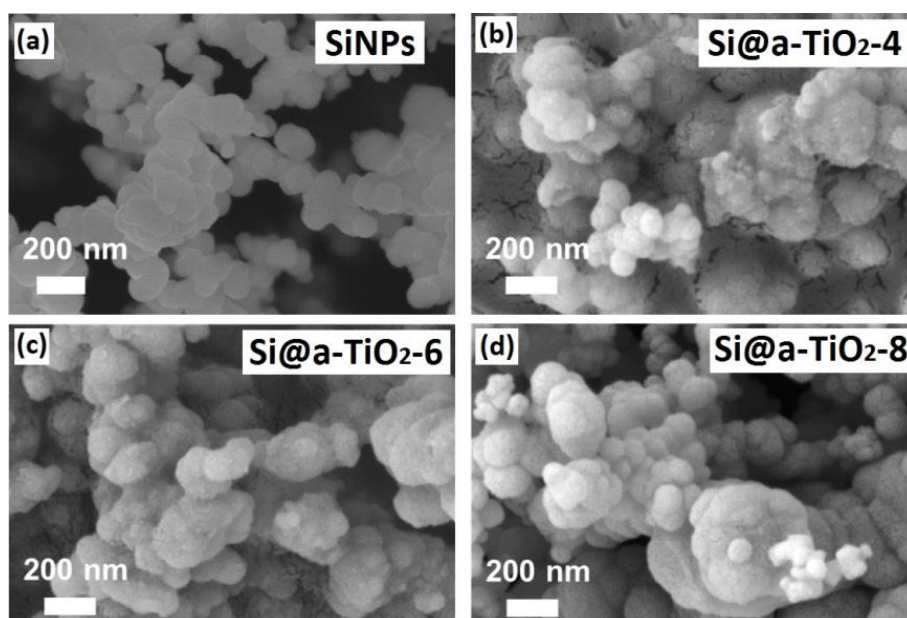


Fig. S1 SEM images of (a) SiNPs, (b) Si@a-TiO₂-4, (c) Si@a-TiO₂-6, and (d) Si@a-TiO₂-8.

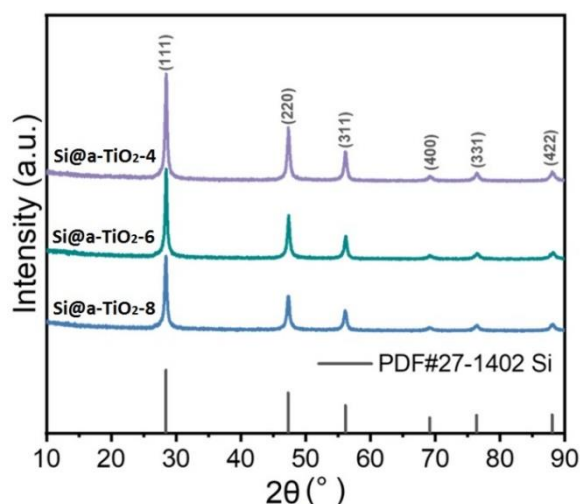


Fig. S2 XRD patterns of Si@a-TiO₂ composites.

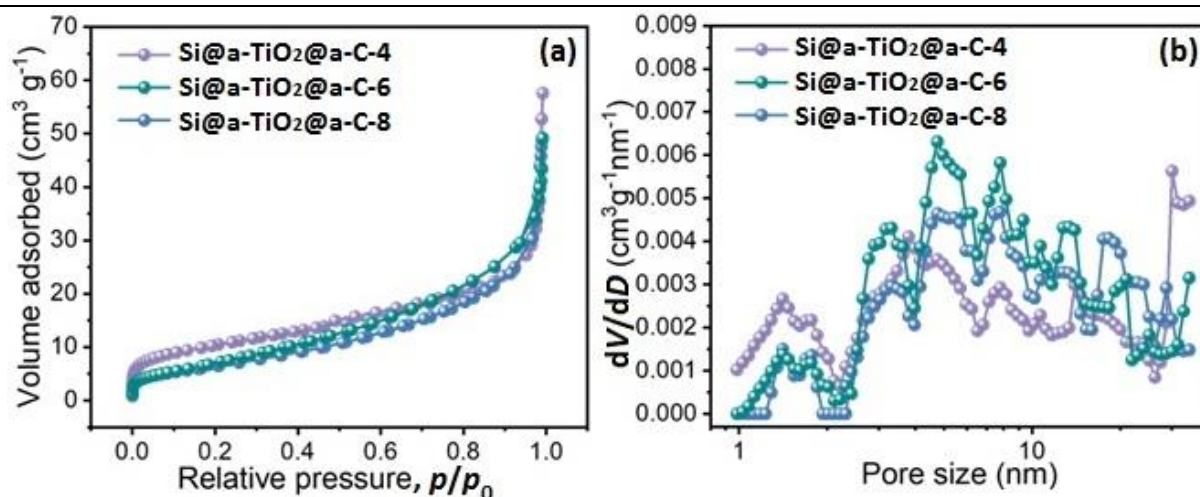


Fig. S3 (a) Nitrogen adsorption–desorption isotherms and (b) pore-size distributions of Si@a-TiO₂@a-C composites.

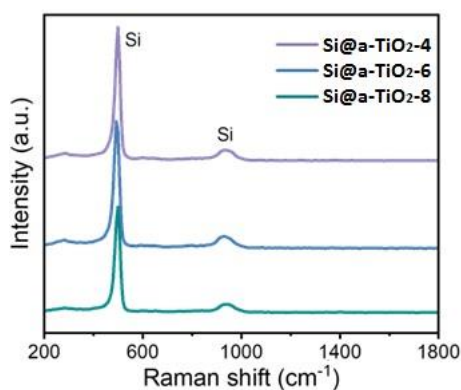


Fig. S4 Raman spectra of Si@a-TiO₂ composites.

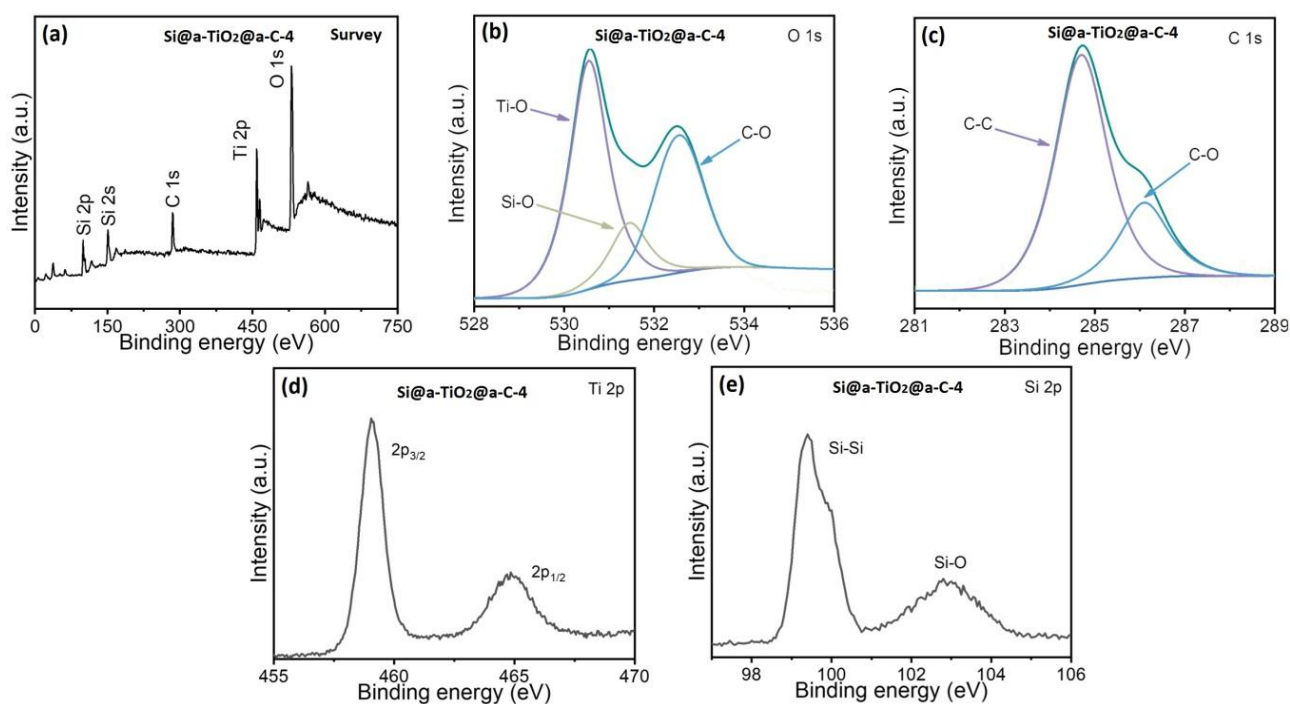


Fig. S5 (a) XPS survey spectrum of Si@a-TiO₂@a-C-4. (b) O 1s, (c) C 1s, (d) Ti 2p, and (e) Si 2p XPS spectra of Si@a-TiO₂@a-C-4.

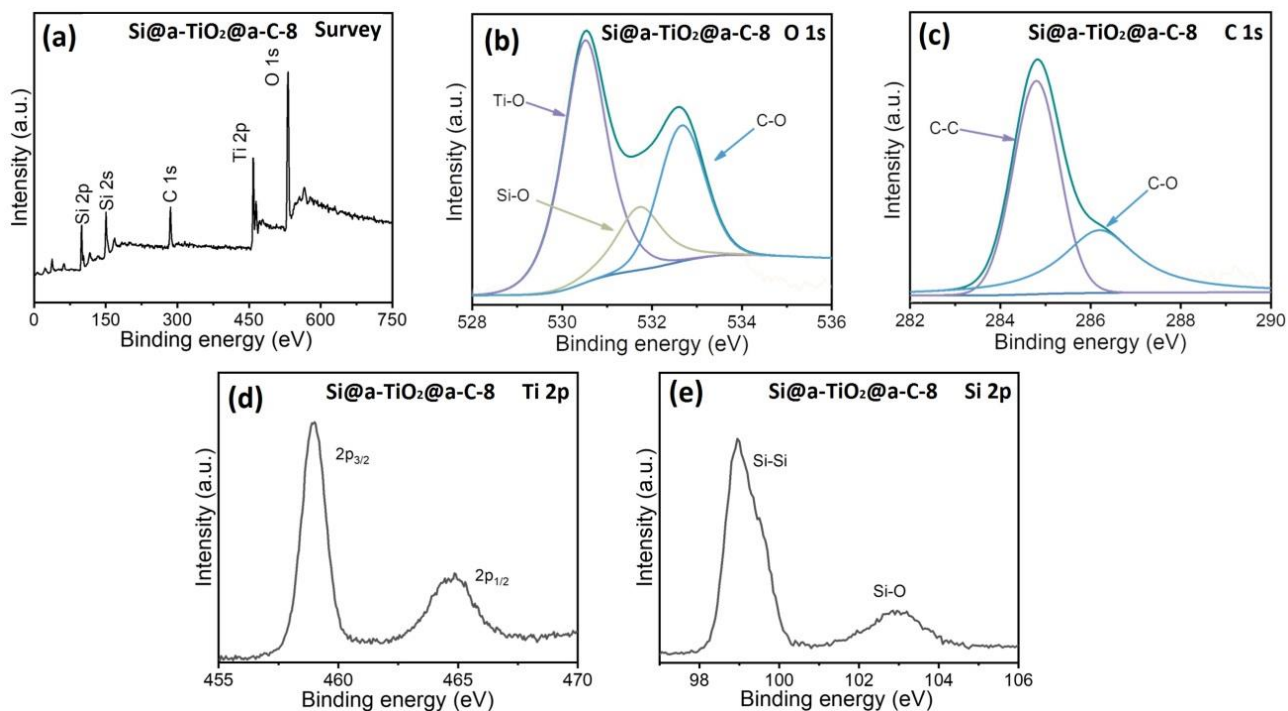


Fig. S6 (a) XPS survey spectrum of Si@a-TiO₂@a-C-8. (b) O 1s, (c) C 1s, (d) Ti 2p, and (e) Si 2p XPS spectra of Si@a-TiO₂@a-C-8.

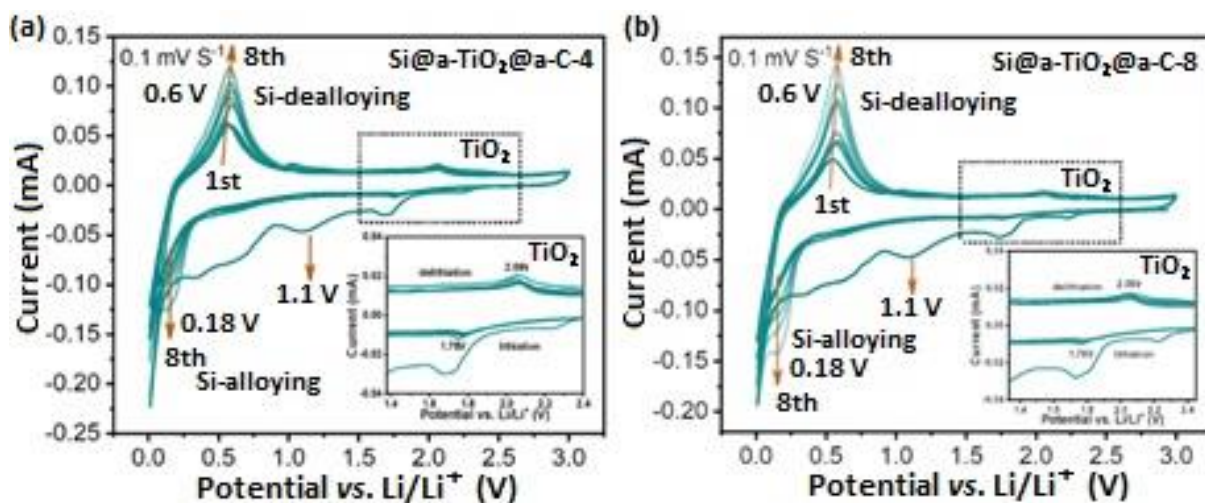


Fig. S7 (a) CV curves of Si@a-TiO₂@a-C-4 at 0.1 mV s⁻¹. (b) CV curves of Si@a-TiO₂@a-C-8 at 0.1 mV s⁻¹.

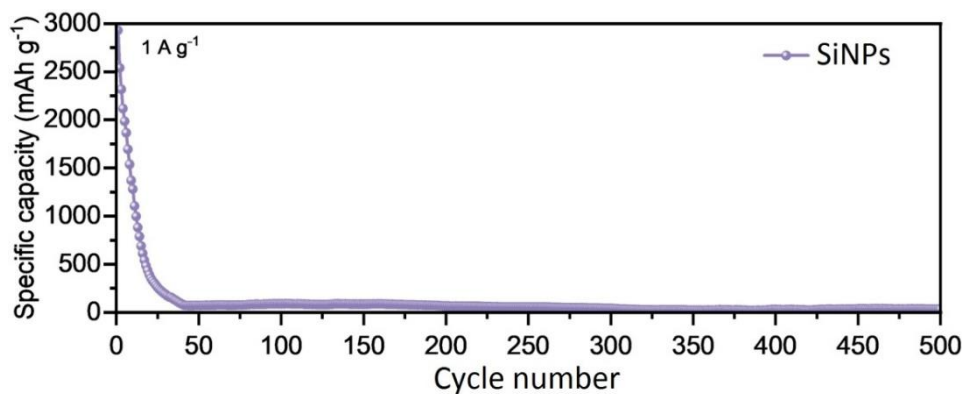


Fig. S8 Cycling performance of the SiNP composite at 1.0 A g⁻¹.

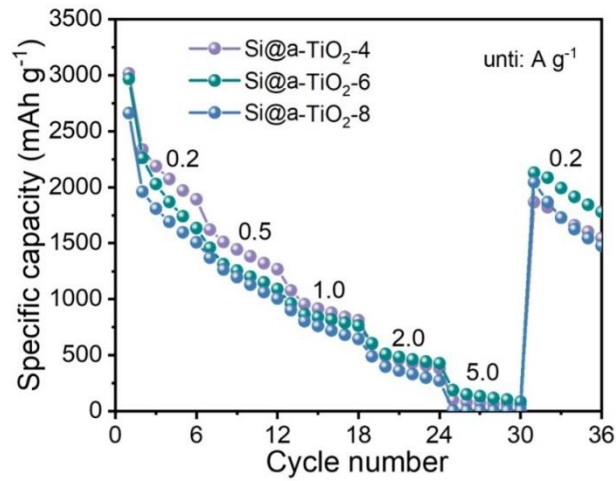


Fig. S9 Rate performance of Si@a-TiO₂ composites at different current densities.

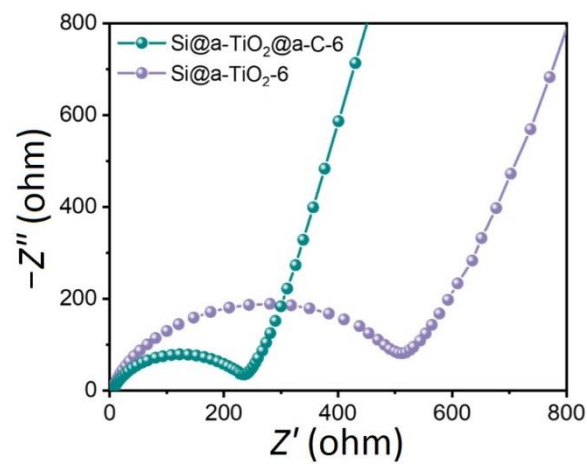


Fig. S10 Nyquist plots of Si@a-TiO₂-6 and Si@a-TiO₂@a-C-6 composites in their initial cycles.

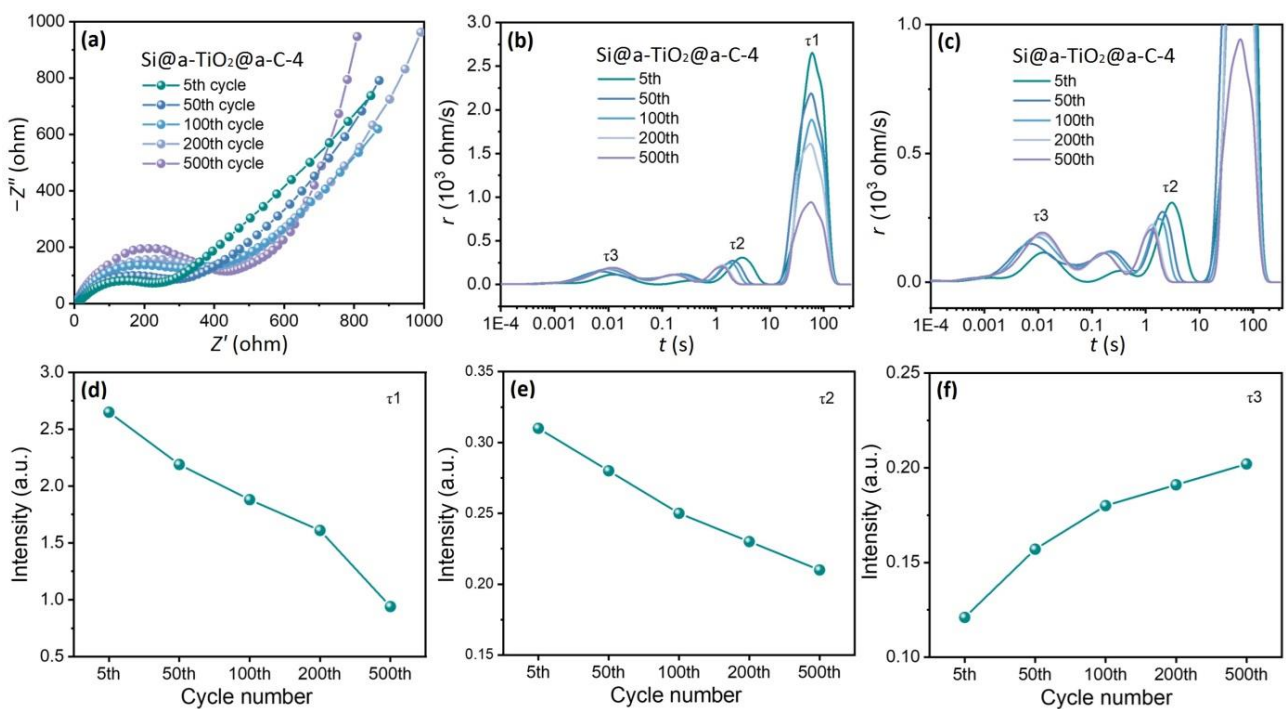


Fig. S11 (a)(b)(c) DRT analysis results obtained from EIS of Si@a-TiO₂@a-C-4 composites. (d)(e)(f) Peak intensity variation trends of τ_1 , τ_2 , and τ_3 .

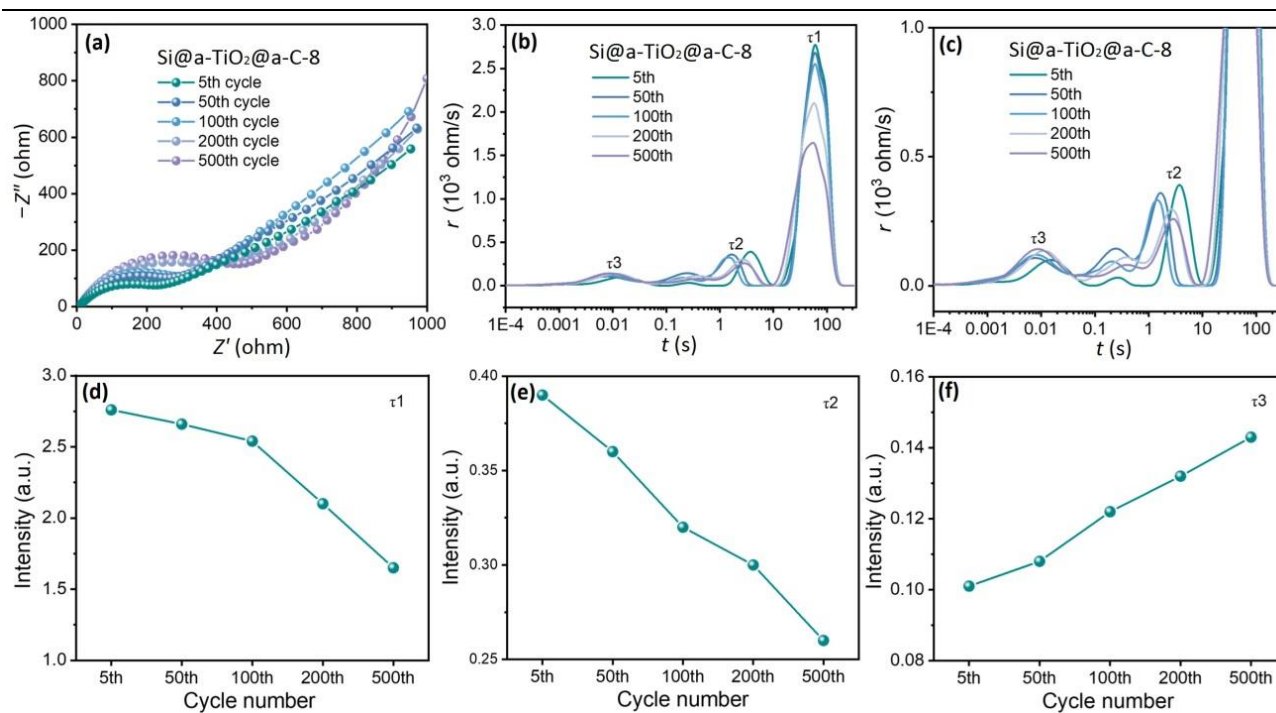


Fig. S12 (a)(b)(c) DRT analysis results obtained from EIS of Si@a-TiO₂@a-C-8 composites. (d)(e)(f) Peak intensity variation trends of τ_1 , τ_2 , and τ_3 .

Table S1 Comparisons in electrochemical performances of different Si-based materials as LIBs anodes

Sb-based material	Current density/(mA·g ⁻¹)	Cycle number	Capacity retention after cycle/(mA·h·g ⁻¹)	Ref.
Si/C	210	300	783	[1]
Nanocrystal-FeSi-embedded Si/SiO _x	1000	1000	491.3	[2]
Si/SiO _x /C	1000	350	886	[3]
Si/G/GF	3579	300	445	[4]
Gr/Si/GO/C	200	100	974.5	[5]
Si/SiC/C	100	220	505.8	[6]
Si@C/rGO	200	100	935.7	[7]
(3D)Si@TiO ₂ @C	500	500	508.9	[8]
SA-SiTc	700	500	1122	[9]
Graphite/Si@TiO ₂	500	100	511	[10]
Si@TiO ₂ @C	2000	100	531.5	[11]
Si@a-TiO ₂ @a-C	1000	500	877.1	This work

References

- [1] Zheng G, Xiang Y, Xu L, et al. Controlling surface oxides in Si/C nanocomposite anodes for high-performance Li-ion batteries. *Advanced Energy Materials*, 2018, 8: 1801718
- [2] He W, Liang Y, Tian H, et al. A facile in situ synthesis of nanocrystal-FeSi-embedded Si/SiO_x anode for long-cycle-life lithium ion batteries. *Energy Storage Materials*, 2017, 8: 119–126
- [3] Yu R, Pan Y, Jiang Y, et al. Regulating lithium transfer pathway to avoid capacity fading of nano Si through sub-nano scale interfused SiO_x/C coating. *Advanced Materials*, 2023, 35: 2306504
- [4] Zhu S, Zhou J, Guan Y, et al. Hierarchical graphene-scaffolded silicon/graphite composites as high performance anodes for lithium-ion batteries. *Small*, 2018, 14: 1802457

- [5] Huang Y, Peng J, Luo J, et al. Spherical Gr/Si/GO/C composite as high-performance anode material for lithium-ion batteries. *Energy Fuels*, 2020, 34: 7639–7647
- [6] Chen Y, Zhang J, Chen X, et al. Facile preparation of Hollow Si/SiC/C yolk–shell anode by one-step magnesiothermic reduction. *Ceramics International*, 2019, 45: 17040–17047
- [7] Li Q, Chen D, Li K, et al. Electrostatic self-assembly bmSi@C/rGO composite as anode material for lithium ion battery. *Electrochimica Acta*, 2016, 202: 140–146
- [8] Hou L, Xiong S, Cui R, et al. Three-dimensional porous carbon framework confined Si@TiO₂ nanoparticles as anode material for high-capacity lithium-ion batteries. *ChemElectroChem*, 2022, 9: 1–10
- [9] Shi J, Zu L, Gao H, et al. Silicon-based self-assemblies for high volumetric capacity li-ion batteries via effective stress management. *Advanced Functional Materials*, 2020, 30: 1–12
- [10] Vats B, Gupta R, Gupta A, et al. Enhancing Li-ion battery performance through the integration of Si@TiO₂ core–shell nanoparticles with natural graphite. *ChemistrySelect*, 2024, 9: e202303545
- [11] Pan Q, Zhao J, Xing B, et al. A hierarchical porous architecture of silicon@TiO₂@carbon composite novel anode materials for high performance Li-ion batteries. *New Journal of Chemistry*, 2019, 43: 15342–15350